AD-A182 558 HIGH TEMPERATURE HOT CORROSION CONTROL BY FUEL ADDITIVES (CONTAMINATED FU..(U) DAVID W TAYLOR NAVAL SHIP RESEARCH AND DEVELOPMENT CENTER ANN.. 1/1

UNCLASSIFIED D V RATHNAMMA ET AL. JUN 87 F/G 11/6.1 NL

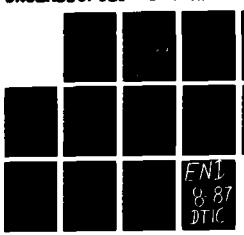

FNL
8-87
DTIC

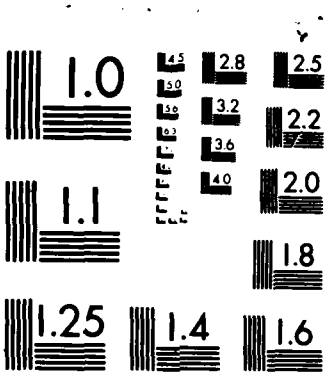

David W. Taylor Naval Ship Research and Development Center
Bethesda, MD 20084–5000

DTNSRDC-SME-87/41 June 1987

Ship Materials Engineering Department
Research and Development

High Temperature Hot Corrosion Control by Fuel Additives (Contaminated Fuels)

by
Dasara V. Rathnamma
David Taylor Naval Ship R&D Center
and
R. Nagarajan
West Virginia University
Morgantown, West Virginia 26505

UNCLASSIFIED
SECURITY CLASSIFICATION OF THIS PAGE

AD-A182558

REPORT DOCUMENTATION PAGE

1a. REPORT SECURITY CLASSIFICATION UNCLASSIFIED	1b. RESTRICTIVE MARKINGS
2a. SECURITY CLASSIFICATION AUTHORITY	3. DISTRIBUTION / AVAILABILITY OF REPORT Approved for public release; distribution is unlimited.
2b. DECLASSIFICATION / DOWNGRADING SCHEDULE Cleared for public release	
4. PERFORMING ORGANIZATION REPORT NUMBER(S) DTNSRDC/SME-87/41	5. MONITORING ORGANIZATION REPORT NUMBER(S)
6a. NAME OF PERFORMING ORGANIZATION David W. Taylor Naval Ship R&D Center 6b. OFFICE SYMBOL (*If applicable*) Code 2813	7a. NAME OF MONITORING ORGANIZATION
6c. ADDRESS (*City, State, and ZIP Code*) Bethesda, MD 20084-5000	7b. ADDRESS (*City, State, and ZIP Code*)
8a. NAME OF FUNDING / SPONSORING ORGANIZATION Office of Naval Research 8b. OFFICE SYMBOL (*If applicable*) R1232	9. PROCUREMENT INSTRUMENT IDENTIFICATION NUMBER
8c. ADDRESS (*City, State, and ZIP Code*) (See reverse side)	10. SOURCE OF FUNDING NUMBERS PROGRAM ELEMENT NO: 63724N PROJECT NO: R0838 TASK NO: R0838SL WORK UNIT ACCESSION NO: DNS 78153

11. TITLE (*Include Security Classification*)
High Temperature Hot Corrosion Control by Fuel Additives (Contaminated Fuels)

12. PERSONAL AUTHOR(S)
Rathnamma, Dasara V. and Nagarajan, R.

13a. TYPE OF REPORT	13b. TIME COVERED	14. DATE OF REPORT (*Year, Month, Day*)	15. PAGE COUNT
Final	FROM Oct 85 TO Dec 86	1987 June	29

16. SUPPLEMENTARY NOTATION
This paper is prepared for presentation at the 10th International Congress on Metallic Corrosion from Nov 7-11, 1987 in Madras, India

17. COSATI CODES		
FIELD	GROUP	SUB-GROUP

18. SUBJECT TERMS (*Continue on reverse if necessary and identify by block number*)
Fuel additives, Blade material, Molten Solution, Thermodynamic corrosion prediction, Chemical equilibrium,
(continued on reverse side)

19. ABSTRACT (*Continue on reverse if necessary and identify by block number*)

The potential of fuel additives to minimize corrosion of blade-material has been analyzed by the following series of steps: first, a computer program was employed for an equilibrium-thermodynamic prediction of condensed solution composition; next relevant physico-chemical properties of the molten solution were estimated based on predicted equilibrium composition; then oxide solubility and dissolution rates are calculated for this solution in contact with various solid oxides. Finally, we compare our predicted oxide dissolution-rate results with available experimental hot corrosion rate data, seeking verification of the model for the rate determining process - i.e., oxide dissolution - in hot corrosion.

20. DISTRIBUTION / AVAILABILITY OF ABSTRACT	21. ABSTRACT SECURITY CLASSIFICATION
☒ UNCLASSIFIED/UNLIMITED ☒ SAME AS RPT ☐ DTIC USERS	UNCLASSIFIED
22a. NAME OF RESPONSIBLE INDIVIDUAL Dasara V. Rathnamma	22b. TELEPHONE (*Include Area Code*) (301) 267-3[illegible]

DD FORM 1473, 84 MAR 83 APR edition may be used until exhausted
All other editions are obsolete
SECURITY CLASSIFICATION OF THIS PAGE

★ U.S. Government Printing Office 1988—539-012

UNCLASSIFIED

(Block 18 Continued)

Oxide solubility,solution properties, Brownian High Schmidt number diffusional flux of oxide, Dissolution rate, Hot corrosion rate, Mass transfer, Concentration gradient, Oxide solvent interface, Multicomponent liquids, Life prediction.

(Block 8c.)

ONR Office of Energy and Natural Resources Technology
Department of the Navy
800 N. Quincy Street
Arlington, Virginia 22217

CONTENTS

	Page
NOTATION	v
ABSTRACT	1
ADMINISTRATIVE INFORMATION	1
INTRODUCTION	1
THEORY OF HOT CORROSION: THE OXIDE DISSOLUTION CRITERION	2
OXIDE DISSOLUTION RATE (ODR) CALCULATION: SINGLE LIQUIDS	3
ODR CALCULATION: MULTICOMPONENT LIQUIDS	6
EFFECT OF ADDITIVES	7
EQUILIBRIUM THERMODYNAMIC PREDICTION OF SOLUTION COMPOSITION	8
ESTIMATION OF SOLUTION/OXIDE DISSOLUTION PROPERTIES BASED ON PREDICTED EQUILIBRIUM COMPOSITION	10
OXIDE SOLUBILITY AND DISSOLUTION RATE CALCULATIONS BASED ON PREDICTED SOLUTION PROPERTIES	11
CORRELATION OF COMPUTED OXIDE DISSOLUTION RATE WITH EXPERIMENTAL HOT CORROSION DATA	13
CONCLUSIONS AND RECOMMENDATIONS FOR FUTURE WORK	17

FIGURES

1. Relative calculated model results for the three binary solutions of the sodium sulfate-vanadium oxide system	12

FIGURES (Continued)

Page

2. Calculated corrosion relative to the no-additive corrosion rate of 910 mg/in^2 x 100 hr. 14

3. Corrosion of 310 alloy with organo-metallic additives..... 15

TABLES

1. NSFO fuel composition for burner rig tests..... 3

NOTATION

Symbol

A	Pre-exponential constant in eq. (4), kg/(ms)
D	Diffusion coefficient, m^2/s
E_μ	Fluidization-energy parameter in eq. (4)
j"o,w	Oxide dissolution flux kg/(m^2 s)
k_m	Mass transfer coefficient kg/(m^2 s)
M	Molecular weight, kg/kg mol
R	Universal gas constant, J/(kg mol K)
s	Streamline distance, m
T	Temperature, K
X	Mole fraction in liquid phase
Λ	Latent heat, of fusion, J/kg mol
μ	Dynamic viscosity, kg/(ms)
ϱ	Density, kg/m^3
σ	Molecular diameter, Å
τ	Shear stress, kg/(ms^2)
ω	Mass fraction

Subscripts

b	Bulk liquid
dp	Dew point
eff	Effective
m	Mass transfer
mp	Melting point
o	Oxide solute

NOTATION (Continued)

sat	Saturation
w	"Wall" / (melt/oxide interface)
1,2	Components 1 and 2 in binary liquid solution
ℓ	Liquid

Mathematical notation

"	per unit area
$\{ \quad \}$	function of

ABSTRACT

The potential of fuel additives to minimize corrosion of blade material in gas turbine engines has been analyzed by the following series of steps: first, a computer program was employed for an equilibrium thermodynamic prediction of condensed solution composition; next relevant physico-chemical properties of the molten solution were estimated based on predicted equilibrium composition; then oxide solubility and dissolution rates were calculated for this solution in contact with various solid oxides. Finally, we compared our predicted oxide dissolution-rate results with available experimental data on hot corrosion rates, seeking verification of the model for the rate-determining process -- i.e., oxide dissolution in hot corrosion.

ADMINISTRATIVE INFORMATION

This work was supported under the Navy Energy Research and Development Program, Mobility Fuels Program Element 63724N, Task Area R0838SL, Work Unit DN578153. The Program sponsor is Dr. Allen Roberts, Office of Naval Research, Code R1232 and the David Taylor Naval Ship Research and Development Center (DTNSRDC) task sponsor is Mr. Richard Strucko, DTNSRDC Code 2759. The work was conducted in the Marine Corrosion Branch.

INTRODUCTION

High chrome steels and superalloys, which are used extensively for high temperature boilers and gas turbine (GT) engines and related components because of their superior high temperature mechanical properties, are susceptible to a form of environmental attack known as "hot corrosion." Hot corrosion is encountered when, for example, liquid (ℓ) Na_2SO_4 is deposited either as a pure phase or in solution with vanadium compounds from combustion gases onto turbine blades and other hot components. Among the factors expected to affect the corrosion resis-

tance of the normally protective oxide coatings are the effective solubilities in the deposited molten salts of protective oxide coatings, and accompanying rate of "dissolution" of the oxide layer. At locations where the oxide scale is partially dissolved, the underlying metal is more accessible, and hence more vulnerable, to corrosive attack.

THEORY OF HOT CORROSION: THE OXIDE DISSOLUTION CRITERION

A model has been developed [1] for life prediction for AISI 310 alloy and Navy special fuel oil (NSFO, composition shown in table 1) based on statistical analysis of an extensive body of data available from burner rig tests covering a wide variety of metallic fuel additives [2]. Although current interest is in superalloys for gas turbine applications, far more data for testing prospective models exist for AISI 310 steel. Further, Cr_2O_3 is the major protective oxide, and more data are available for that oxide than for other oxides which play an important role in protective coatings of superalloys. This research [2] has concentrated on understanding the aggravating effects of trace vanadium in the fuel, and relatively little data are available for model comparison with superalloy corrosion.

The approach described in this paper was to develop a model from theoretical principles and then verify it by comparison with the experimental results, the emphasis being on modeling the effect of fuel additives on hot corrosion. Our modeling of the rate of the hot corrosion process is based on the following important hypothesis [3]: There is a strong correlation between regions on a blade where the predicted oxide dissolution rate is high and regions which ultimately exhibit severe hot corrosion. Corrosion "maps," which have been reported for a few test turbine blades [4], have been found to agree reasonably well with our predicted relative oxide dissolution rate (RODR) profiles for the same blade.

Table 1. NSFO fuel composition for burner rig tests.

Carbon (wt%)	87.2
Hydrogen (wt%)	10.8
Sulfur	1.83
Water & Sediment (wt%)	0.10
Ash (wt%)	0.043
Vanadium (ppm)	170
Sodium (ppm)	22
Other Metals (ppm)	47
Heating Value (Btu/lb)	18,617

OXIDE DISSOLUTION RATE (ODR) CALCULATION: SINGLE LIQUIDS

We assume the oxide dissolution rate in the flowing molten salt solvent layer (solution) to be limited by the rate of oxide (solute) diffusion from the oxide/solvent interface to the bulk-liquid. The Brownian high-Schmidt number diffusional flux of oxide into the liquid may be represented as a product of a mass transfer coefficient and a concentration gradient:

$$j''_{o,w} = k_m \cdot (\omega_{o,w} - \omega_{o,b}) \quad . \qquad (1)$$

Where ω_o is the oxide mass fraction at the melt/oxide interface (ω) or in the bulk liquid solution b, and k_m, the mass transfer coefficient,* is estimated to be:

* Our convective diffusion mass transfer approach to the prediction of the steady-state oxide dissolution rate is patterned after that of Stewart [11].

$$k_m = 0.53837 \frac{D_{o,\ell}\,\varrho_\ell}{[D_{o,\ell}(\frac{\tau_w}{\mu_\ell})^{-3/2} \int_o^{\ell_s} (\tau_w/\mu_\ell)^{1/2} ds]^{1/3}} \quad . \tag{2}$$

The Brownian diffusion coefficient, $D_{o,\ell}$, of the oxide solute in the condensed liquid is calculated according to the Stokes-Einstein equation [5]:

$$D_{o,\ell} \cong \frac{k\,T_w}{3\pi\mu_\ell\,\sigma_{o,eff}} \quad . \tag{3}$$

where k is the Boltzmann constant, T_w is the local blade surface temperature, μ_ℓ is the viscosity of the liquid phase, and $\alpha_{o,eff}$, the effective size of the solute molecule in the solvent, is tentatively estimated as the "hard-sphere" diameter of the corresponding metal element (e.g., Cr in the case of Cr_2O_3 - protective coating).** Molten sulfate, vanadate and oxide viscosities have been measured over a wide temperature range [6,7] and can be expressed as a function of temperature in the following activation-energy formulation:

$$\mu_\ell(T_w) = A \exp(-E_\mu/T_w) \quad . \tag{4}$$

Other factors involved in the estimation of k_m (eq. (2)) include the liquid density, ϱ_ℓ, and the shearing stress due to the mobile liquid layer, τ_ω. Condensate layer flow due to gas aerodynamic, centrifugal (in the case of rotor blades), and surface-tension shear forces provide a continuous "fluxing" mechanism by which fresh solvent is supplied to the dissolution site and the dissolved oxide is transported away toward the tip and trailing edge of the blade [8]. This appears to be a more logical framework to explain why the melt does not saturate

** In view of the limited experimental data and consequent uncertainty regarding the identity of the oxide species in solution, we here estimate in effect its "maximum" diffusion coefficient in order to provide a safe or conservative estimate of life.

locally with the oxide than proposed explanations involving local oxide dissolution/reprecipitation processes sustained, by a negative (normal) gradient of oxide solubility at the oxide/salt interface [9], or by a thermally-induced surface tension gradient [10].

The integral in the denominator of the right-hand side of eq. (2) is to be performed along streamlines of the shear-driven condensate flow. Thus s stands for the streamwise distance. The oxide mass fractions in the liquid that provide the concentration gradient for the dissolution process are estimated as follows: The oxide saturation mass fraction at the melt/oxide interface, $\omega_{o,w,}$ is taken to be the following "ideal-solubility" ("saturation") value [12] in the absence of inherent interfacial kinetic limitations to the maximum local dissolution rate [13]

$$\omega_{o,w} = \omega_{o,w,sat} \cong \frac{M_o}{M_\ell} \exp\left(\frac{\Lambda_o}{R} \cdot \left(\frac{1}{T_{mp,o}} - \frac{1}{T_w}\right)\right) . \qquad (5)$$

M_o and M_ℓ are the molecular weights of the oxide and liquid, respectively; Λ_o is the latent heat of oxide fusion, R the universal gas constant, and $T_{mp,o}$ is the melting-temperature of the oxide. For a given oxide/solvent combination, this saturation mass fraction is then a function only of local surface temperature. However, the oxide mass fraction in bulk liquid, $\omega_{o,b}$, depends on the relative rates of local solvent deposition and solute dissolution, as well as the streamline inflow of material from upstream locations. In the present analysis, we assume that $\omega_{o,b}$ is negligible compared to $\omega_{o,w}$, thereby suppressing a major flow effect but biasing for maximum dissolution rates, which are of interest to design engineers.

ODR CALCULATION: MULTICOMPONENT LIQUIDS

Once physico-chemical properties of pure liquids, e.g., Na_2SO_4, $NAVO_3$, and V_2O_5, have been obtained, properties of ideal multicomponent solutions between these may subsequently be approximated as arithmetic (weighted) means of the constituent properties, i.e.,

$$\begin{aligned} \varrho_\ell &\cong X_1 \varrho_{\ell,1} + X_2 \varrho_{\ell,2} \\ \mu_\ell &\cong X_1 \mu_{\ell,1} + X_2 \mu_{\ell,2} \\ M_\ell &\cong X_1 M_{\ell,1} + X_2 M_{\ell,2} \end{aligned} \qquad (6)$$

where 1 and 2 are the components in a binary solution, and X's represent liquid compositions. The effect of nonideality, neglected here, can be incorporated as a correction factor that is related closely to the heat of mixing [14].

The composition dependence of a solution's freezing point is determined from available phase diagrams [15], and may also be obtained using computer programs written to generate phase diagrams (e.g., POTCOMP [16]). The effect of lowering the melting point of solution condensates below the pure-component values is important in view of the fact that solid condensed phases on turbine blades are relatively benign with respect to hot corrosion. Typical illustrations of this effect are low-temperature hot corrosion by $CoSO_4$ - Na_2 SO_4 mixtures [17] and corrosion by Na_2SO_4 - V_2O_5 - $Na_2V_2O_6$ solutions in gas turbines burning liquid fuels containing sodium and vanadium [18,19].

In addition to lowering the freezing point, solution-forming contaminants increase the solution dew point, thereby further widening the potentially dangerous temperature interval (T_{dp} - T_{mp}) in which hot corrosion can occur. Introduction of a second trace species can potentially lower the vapor pressure of the

primary species at the gas/condensate interface (w) if the introduced species forms a solution condensate with primary species, and the effect would increase the vapor-diffusional flux of that species toward (w). In our present theory, single species diffusional deposition fluxes, e.g., Na_2SO_4 (ℓ) on the surface, are taken as single vapor (precursor, e.g., $Na_2SO_4(g)$) concentration diffusion through a chemically frozen boundary layer (CFBL). In the multicomponent case, individual constituents still deposit by single species vapor diffusion, but their molar fluxes have to be in the same ratio as their mole fractions in the condensed phase. A more detailed discussion of these aspects, and other considerations and limitations of the total deposition rate calculation is available elsewhere [3,5,8,13]. The theoretical rate, j"o,m, (see figures 1a-c) is scaled proportionally by deposition rate calculated on the basis of trace vapor diffusion model.

EFFECT OF ADDITIVES

Modeling the effect of fuel additives in hot corrosion environments involves the following steps: (1) Calculate equilibrium thermodynamic compositions of the condensed solutions; (2) Obtain or estimate necessary physico-chemical properties of the molten equilibrium solutions; (3) Model oxide solubilities and dissolution rates for the various solid oxides in contact with the equilibrium solution, and (4) Compare the predicted oxide dissolution rates with available experimental data to verify this oxide dissolution model for the rate-determining process in hot corrosion.

EQUILIBRIUM THERMODYNAMIC PREDICTION OF SOLUTION COMPOSITION

The complex Chemical Equilibrium Calculation (CEC) computer program developed at NASA Lewis Research Center (LeRC) [20] makes use of an extensive thermodynamic database and an efficient free-energy minimization algorithm to make local thermochemical equilibrium (LTCE) calculations of gas and liquid compositions at assigned temperature, pressure, and elemental ratios, for example, of the fuel entering a combustor [21]. While a few generally available computer programs [22] apparently have the ability to consider solutions at other than unit activity of the components, they are unsuitable for computations of mixtures as complex as Navy fuel. Calculation of solutions at realistic activities is essential to avoid completely erroneous thermodynamic predictions. The NASA CEC program is being modified at LeRC* and the current version, which treats ideal solution condensates, was used here to compute solution compositions. The LeRC solution-capable version of the CEC code certainly has limitations in its present form -- e.g., singular matrices are sometimes encountered when condensed phases are added, or reintroduced as the temperature is lowered from an all-vapor state; the code occasionally fails to converge, getting caught in an infinite cycle of condensed phase additions and removals. Avoiding these problems requires care. More serious is a failure to model the physical state in that the database form requires use of the most stable pure phase thermodynamic functions for all components in a solution. This results in the curious inclusion of solid species in a liquid

* F.J. Zeleznik, unpublished work, National Aeronautics and Space Administration, Lewis Research Center, Cleveland, Ohio (1986)

solution. However, for this work, the temperatures considered are above, or near, all liquidus temperatures, so this problem is minor. In many respects, however the CEC code is still more robust than many other free-energy minimization codes, e.g., it aggressively selects the atomic/molecular basis to improve convergence and avoid singularities. It has been deliberately optimized to improve accuracy for parts-per-million level trace species. The CEC was used to compute mole fractions.

Equilibrium thermodynamic calculations were performed at a surface temperature of 1144 K and at atmospheric pressure. The additive level is expressed as the atomic ratio of metal additive to vanadium in the fuel. Results indicate that all additives considered tend to increase the mole fraction of Na_2SO_4 (ℓ) in solution, by preferentially forming gaseous and solid compounds with the vanadium present. Potassium, sodium, barium, iron, lead, and magnesium induce the greatest enrichment of the sulfate in the condensed phase, whereas introduction of Zn, Al, Nd, and Ce leads to least sulfate enrichment. The concentration of the corrosive sodium vanadate is reduced since vanadium forms vanadates with additive metals.

The phase fraction of entire condensed material as a function of the additive's metal concentration was also obtained from CEC calculations (plots not shown here). Except for Na and Zn, all other additives tend to depress the amount of condensed solution that forms. The less the amount of deposition of molten liquid phases, of course, the less the extent of hot corrosion initiated by oxide layer dissolution. It is worth noting that while nearly all additives considered here are quite effective in reducing net deposition of the molten phase, increasing the additive concentration beyond a certain level -- usually corresponding to a metal-to-vanadium atom ratio of about 2 -- is at best marginally successful, and often clearly counter-productive. Another interesting

observation is that zinc appears to be a "bad" additive based on this observation; however, a closer examination of condensed species formed reveals that the additional deposit is made up almost entirely of solid zinc vanadates which corrode surfaces only to a negligible extent. An analysis of the effect of metal additive concentration on Na_2SO_4 (ℓ) condensation indicates that the total amount (product of mole fraction and phase fraction) of Na_2SO_4 (ℓ) which condenses is raised to the greatest extent by zinc, barium, iron, and magnesium additives, whereas cerium, aluminum and nickel have the least effect.

ESTIMATION OF SOLUTION/OXIDE DISSOLUTION PROPERTIES BASED ON PREDICTED EQUILIBRIUM COMPOSITION

Having acquired ideal solution composition data by using the CEC (solution) program, we proceed to estimate solution properties, such as density, viscosity and molecular weight, by the simple approximate "rules" stated in eq. (6). Among the pure liquids, considered here, Na_2SO_4 (ℓ) is the least dense and least viscous; $NaVO_3$ (ℓ) is the most viscous and V_2O_5 (ℓ) has the highest molecular weight and is most dense. Thus, in a Na_2SO_4 (ℓ) - $NaVO_3$ (ℓ) binary ideal solution, with increasing Na_2SO_4 (ℓ) concentration, the solution molecular weight increases, while the density and viscosity decrease; in a $NaVO_3$ (ℓ) - V_2O_5 (ℓ) solution with increasing $NaVO_3$ (ℓ) concentration, molecular weight and density decrease while viscosity increases; in the third binary solution in this ternary system, Na_2SO_4 (ℓ) - V_2O_5 (ℓ), with increasing Na_2SO_4 (ℓ) concentration, molecular weight, density and viscosity of the solution decrease.

OXIDE SOLUBILITY AND DISSOLUTION RATE CALCULATIONS BASED ON PREDICTED SOLUTION PROPERTIES

An examination of eqs. (2), (3) and (5) indicates that the dissolution rate of a given oxide* should increase with

- decreasing liquid viscosity,
- increasing liquid density, and
- decreasing liquid molecular weight.

As the liquid phase composition changes, the oxide dissolution rate responds to physical-property changes acting in concert. The resulting relative oxide dissolution rate, liquid deposition rate, and oxide saturation mass fraction in solution profiles are plotted against composition for the three ideal binary solutions in figures 1a, 1b, and 1c. In solutions of Na_2SO_4 (ℓ) with $NaVO_3$ and V_2O_5, as the sulfate mole fraction increases, so does the oxide dissolution rate; however, the oxide solubility decreases with increasing Na_2SO_4 (ℓ) mole fraction in the Na_2SO_4 - $NaVO_3$ solution and increases with Na_2SO_4 (ℓ) mole fraction in Na_2SO_4 - V_2O_5 solution. Thus a simplistic viewpoint of oxide solubility as the key factor in determining hot corrosion rates may lead to serious errors in analysis should our more general dissolution-rate criterion, which incorporates in it the oxide solubility, prove to be more relevant. In the case of the $NaVO_3$ - V_2O_5 liquid solution, the oxide mass fraction in the solution increases with increasing mole fraction of $NaVO_3$ (ℓ), whereas the relative oxide dissolution rate decreases to a small extent initially,

* When comparing different oxide species, smaller, faster-diffusing molecules of greater molecular weight, greater latent heat of fusion, and lower melting point appear to dissolve readily in a given molten-solvent liquid phase.

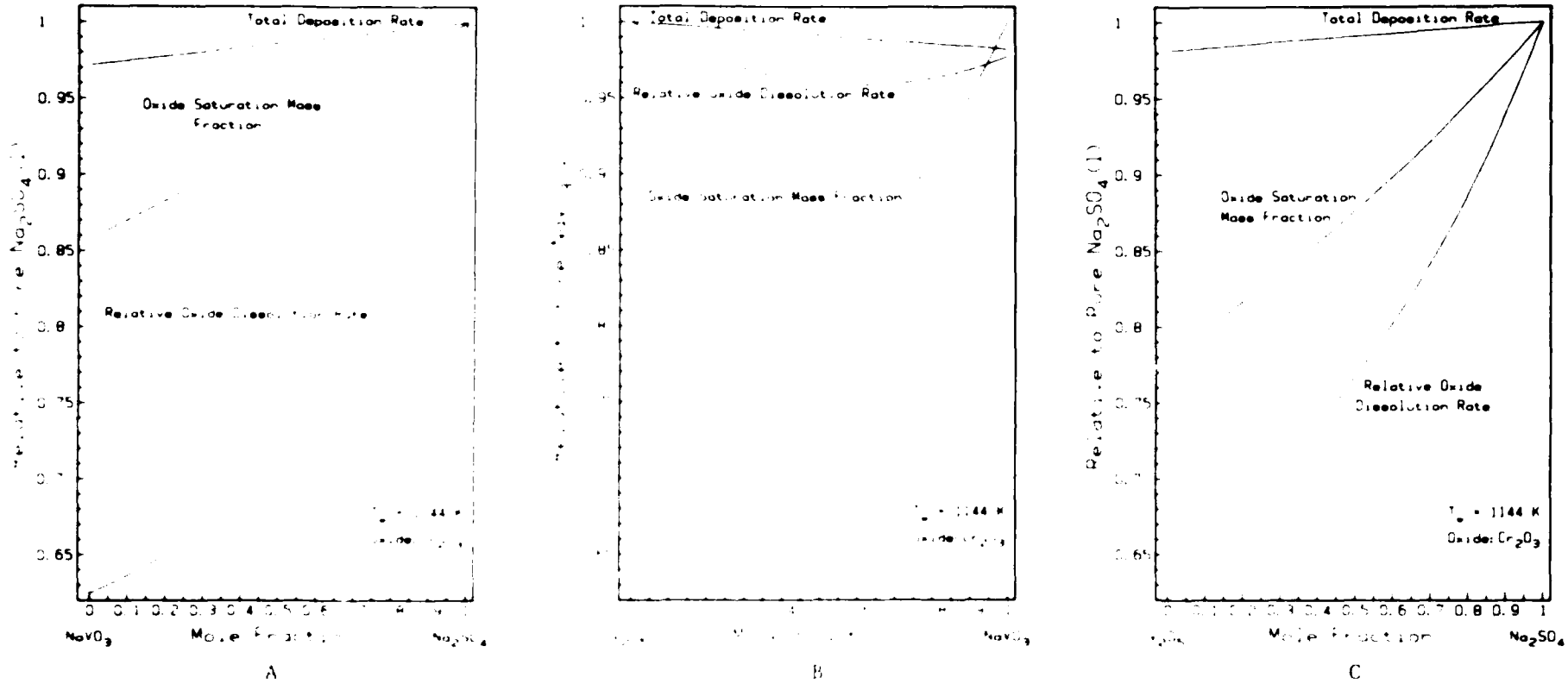

Fig. 1. Relative calculated model results for the three binary solutions of the sodium sulfate-vanadium oxide system. The line labeled Total Deposition Rate is calculated from CFBL (see text) considerations and represents the change in solution composition change. The Oxide Saturation Mass Fraction (eq. 5) is relative to the value in the pure liquid endmember. Relative Oxide Dissolution Rate is from eq. (1). Values were determined at T_w (surface temperature) = 1144 K (1600 F) for dissolution of Cr_2O_3.

and then increases slowly. The effect of composition change on the total solution deposition rate is minimal because the surface temperature is very low, presumably well below the dewpoint for the solution.

CORRELATION OF COMPUTED OXIDE DISSOLUTION RATE WITH EXPERIMENTAL HOT CORROSION DATA

The corrosion rate with no additive for a 310 alloy in a turbine burning Navy special grade fuel (see Table 1 for its composition) has been reported at 1600° F (1144 K) by Schab [2] to be 910 mg/inch^2/100 hours. This number is divided by the calculated oxide dissolution rate value in the presence of the appropriate liquid condensed phase and (no-additive) fuel make-up reported in table 1, to obtain a scale-up factor. Subsequent oxide dissolution rate predictions were multiplied by this scale-up factor in order to compare them directly with reported hot corrosion data. In figures 2a, 2b, and 2c, we present scaled-up corrosion rates (computed values based on our oxide dissolution rate model) as a function of metal additive-to-vanadium atom ratio. In figure 3 we have reproduced the experimental results of Schab [2] pertaining to hot corrosion of 310 alloy in the presence of organo-metallic salt additives. Predicted trends indicate that magnesium, cadmium, cobalt, manganese, and nickel additives were the most effective suppressants of dissolution-controlled hot corrosion, whereas cerium and aluminum were among the less effective. Added sodium tends to enhance the corrosion rate considerably with respect to its zero-additive value; this appears reasonable in view of the fact that added sodium increases deposition rate of the condensed solution, as well as the fraction of sodium sulfate in it. In addition, this prediction is in agreement with other reports of Na involvement in corrosion. However, most such reports are for Na at a few ppm. High sodium concentrations

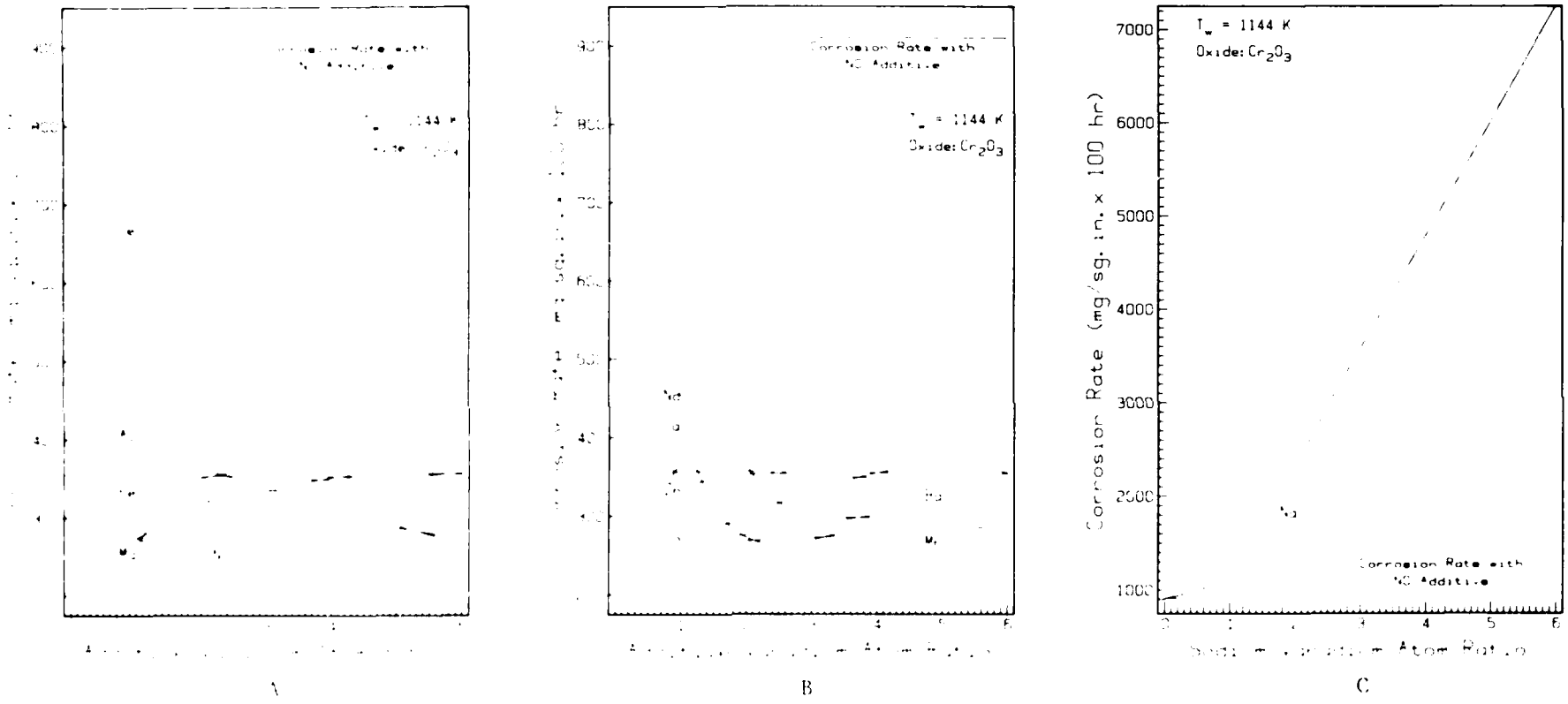

Fig. 2. Calculated corrosion relative to the no-additive corrosion rate of 910 mg/in^2 x 100 hr. Values have been calculated at metal/vanadium atom ratios of 1 to 6, and splined to indicate trends.

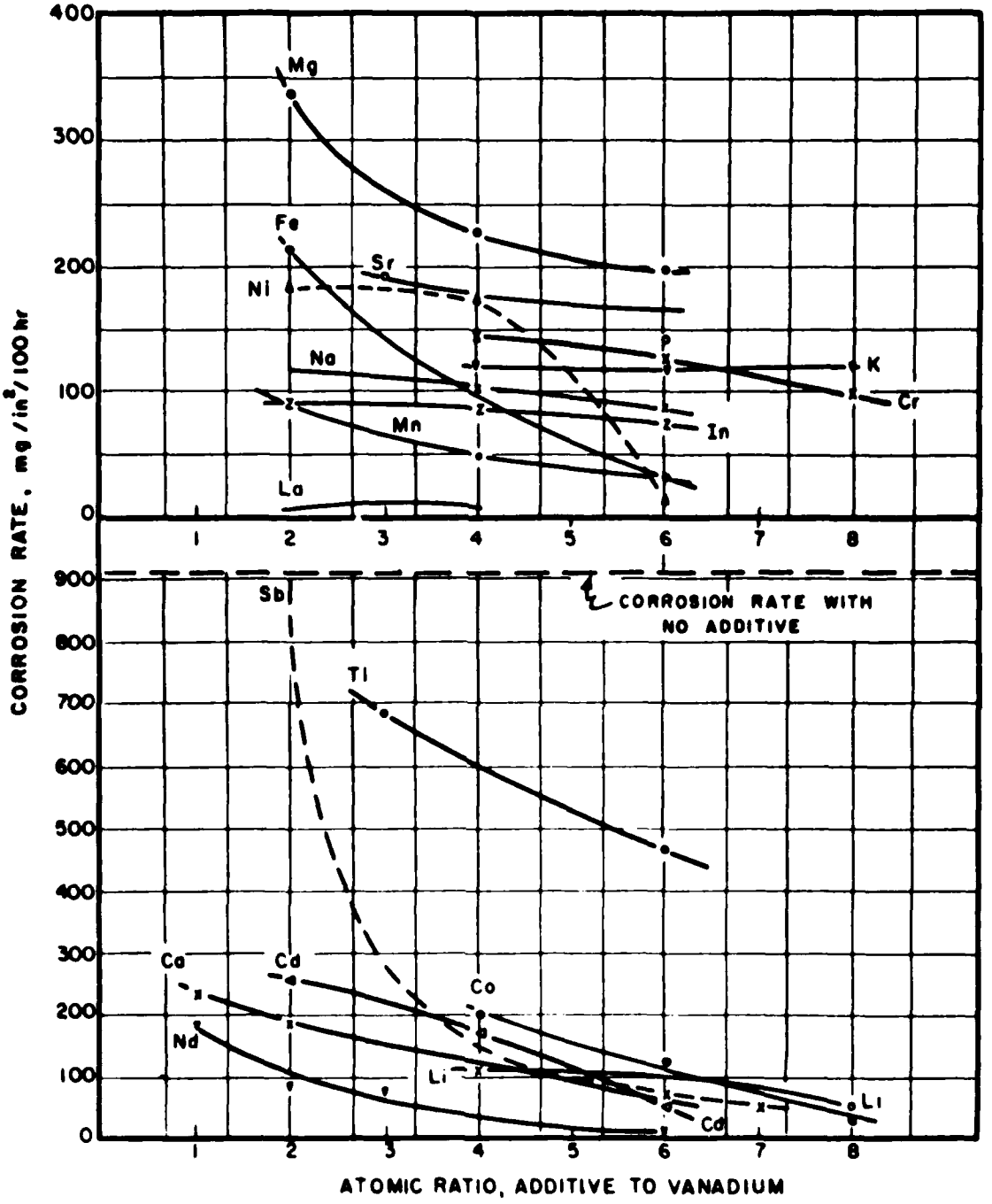

Fig. 3. Corrosion of 310 alloy with organo-metallic additives. Fuel -- Navy Special Grade; Temperature -- 1144 K (1600°F).

results reported by Schab [2] have also been reported elsewhere in literature [19]. Agreement between experimental hot corrosion rate results and our model predictions for the corrosion rate based on an oxide-dissolution criterion is encouragingly good; especially in a qualitative sense. Indeed, as per our theory, Mn, Cd, Co, Ni, Mg and Fe are found to be effective inhibitors of hot corrosion. There is a discrepancy between theory and experiments in the case of Na and K additives; potassium apparently has little influence on hot corrosion rates when used as an additive, and added sodium apparently decreases rates. These results are contrary to our findings. Perhaps, future refinements in our theory for hot corrosion and in the corrosion test procedures to obtain rate data would provide a closer match between theoretical expectations and experimental realizations.

In quantitative terms, predicted and observed corrosion rates are in closest agreement for tests involving magnesium, iron, cobalt, and nickel as additives, and in poorer agreement for sodium, potassium, and lanthanum additives. For some additives, e.g., Nd, La, Mn, experiments indicate a far greater corrosion suppression effect than the model predicts. Both experiments and model predictions show a leveling off in the reduction in corrosion rate beyond a certain concentration of the additive, but the leveling predicted by our model begins sooner (at an additive-to-vanadium atomic ratio of about 1 to 1.2) than observed experimentally. In addition, the predicted corrosion rate curves turn up eventually, corresponding to additive concentrations which continue to enrich the solution in the sulfate after an asymptotic limit to the total condensed-phase fraction has been reached. This behavior is not manifested by experimental hot corrosion rate data.

he following steps are expected to improve the agreement between theoretical model predictions and the experimental results [3]. First, instead of a single vapor diffusional model, the model can include multicomponent transport for boundary layer deposition suitable for the marine environment. Kinetic limitations to interfacial oxide/solvent rate process, if incorporated will reduce the maximum diffusion controlled oxide dissolution rate [8]. Also, additional experiments should be performed with modified additives which include compounds to deliberately promote or prevent the nucleation of inorganic condensates (aerosols). In addition, the CEC code needs improvement. Having more accurate thermodynamic data for all of the vanadium compounds used in the computer calculations is certainly the key to obtaining more accurate results. It is important to remember that the burner rig is not a research instrument and the corrosion measurements are only approximate. And finally, the estimation process is to be refined by using better support data like viscosities, shearing stresses and densities.

CONCLUSIONS AND RECOMMENDATIONS FOR FUTURE WORK

The work presented here represents a new major effort to study the interrelated problems of molten-condensate deposition and subsequent hot corrosion. It is an attempt to apply a theoretically-based model of the deposition process, coupled with a thermodynamic equilibrium solution-based calculation of the liquid deposit to permit a dynamic dissolution model calculation. Previous work in this area has been confined predominantly to statistical regression analyses, coupled with simplified mechanistic models. The use of regression analyses to identify significant parameters or to provide working correlations has its values for analyzing the quality of experimental data as well as in identifying sensitive

model parameters. However, corrosion data continues to be accumulated at a steady pace, and unless theoretical or computer-modelling based efforts are undertaken, analyses of the data will remain a collection of empirical correlations. Several possible improvements in the theory presented here have been discussed elsewhere in other applications [8], and will be incorporated as data become available. Identification of underlying theoretical frameworks can only improve the use of such methods in analysis of experimental data. The use of local thermodynamic equilibrium codes, such as the NASA LeRC CEC code used here, to predict gas and liquid phase compositions, and the development of a mass transfer model to predict the rate of oxide dissolution into the liquid phase constitute the first steps in what will undoubtedly be a continuous process of model refinement on the basis of feedback obtained from comparison with hot corrosion test data. The long term goal of this research is life prediction for turbine blades used in hot corrosive environments.

ACKNOWLEDGEMENT

The authors acknowledge Dr. David W. Bonnell for critical reading of this manuscript. This work was supported by the Fuel Qualification Procedure Project (FQP), funded by the United States Navy's Office of Naval Research. The program sponsor is Allen Roberts, Code R1232, Energy and Natural Resources Technology Office, Washington, D.C.

REFERENCES

1. Rathnamma, D. V. and D. W. Bonnell, "Contaminated Fuel Combustion and Material Degradation Life Prediction Model," Proc., High Temperature Alloys for Gas Turbines and other Applications, W. Betz et al, editors, D. Reidel Publishing Company, p. 1105-1116 (1986).

2. Schab, H. W. and Frank R. Gessner, "Reduction of Oil-Ash Corrosion by Use of Additives in Residual Fuels," United States Naval Engineering Experiment Station, Research and Development Report 070034C, NS-072-504 (17 Apr 1957).

3. Rosner, D. E. and R. Nagarajan, "Vapor Deposition and Condensate Flow on Combustion Turbine Blades: Theoretical Model to Predict/Understand Some Corrosion Rate Consequences of Molten Alkali Sulfate Deposition in the Field or Laboratory," Int. J. Turbo Jet Engines (1987) (in press).

4. Fryxell, R. E. and I. I. Bessen, "Coating Life Assessment in Gas Turbines Operated for Ship Propulsion," in: Proc., of 1974 Gas Turbine Materials in the Marine Environment Conf., 24-26 Jul, 1974 J. W. Fairbanks, editor, Marine Maritime Academy, Castine, Maine, p. 259-276 (1974).

5. Rosner, D. E., Transport Processes in Chemically Reacting Flow Systems, Butterworth Publishers (1986).

6. Cutler, A.J.B., "Molten Sulfates," in: Molten Salt Techniques, Plenum Press (1983).

7. Janz, G. J., Molten Salts: vol. 5, Part 2. Additional Single and Multi-Component Salt Systems; Electrical Conductance, Density, Viscosity and Surface Tension Data, J. Phys. Chem. Ref. Data 12, p. 591-815 (1983).

8. Nagarajan, R., "Theory of Multicomponent Chemical Vapor Deposition (CVD) Boundary Layers and Their Coupled Deposits," Dissertation Thesis, Dept. of Chemical Engineering, Yale University (May, 1986).

REFERENCES (Continued)

9. Rapp, R. A. and K. Goto, in: Proc., Fused Salt Symp. II, J. Braunstein, editor, The Electrochemical Society, Princeton (1979).

10. Lau, K. and S. C. Singhal, "Fluxing of Protective Oxide Scales on Superalloys via a Thermal Surface Tension Gradient," Westinghouse R&D Center, 82-104-Metal-PI (1982).

11. Stewart, W. E., "Convective Heat and Mass Transport in Three-Dimensional Systems with Small Diffusivities," Physiochemical Hydrodynamics, vol. 1, p. 23-63 (1977).

12. Denbigh, K. G. and J.C.R. Turner, Principles of Chemical Equilibrium, second edition, p. 267, equation 8-83 (1966).

13. Rosner, D. E. and R. Nagarajan, "Transport Induced Shifts in Condensate Dew-Point and Composition in Multicomponent Systems With Chemical Reaction", Chem. Eng. Sci., vol. 40 p. 177-186 (1985).

14. Moelwyn Hughes, E. A., Physical Chemistry, second edition, Pergamon Press (1964).

15. Phase Diagrams for Ceramists, vol. I-V. 1964-1983. Compiled at the U.S. National Bureau of Standards. Edited and published by the American Ceramic Society.

16. Bale, C. W., A. D. Pelton, and W. T. Thompson, F*A*C*T (Facility for the Analysis of Chemical Thermodynamics) User's Guide, McGill University/Ecole Polytechnic, Montreal, Quebec, Canada (1979).

17. Jones, R. L., "Hot Corrosion in Gas Turbines," Proc., of the Symp. on Corrosion in Fossil Fuels Systems, vol. 83-5, Electrochemical Society, Pennington, N.J., (1983).

18. Luthra, K. L. and H. S. Spacil, "Impurity Deposits in Gas Turbines from Fuels Containing Sodiumm Vanadium," J. Electrochem. Soc, Solid-State Sci. Tech. p. 649-656 (1982).

19. Lahiri, A. K., H. R. Thilakan, and T. Banerjee, "Oil-Ash Corrosion of Alloy Steels at High Temperatures," Proc., 4th Int. Conf. on Metallic Corrosion, N. E. Hamner, editor, National Association of Corrosion Engineers p. 269-270 (1969).

20. Gordon, S. and B. J. McBride, "Computer Program for Calculation of Complex Chemical Equilibrium Compositions, Rocket Performance, Incident and Reflected Shocks, and Chapman-Jouguet Detonations," NASA SP-273, Interim Revision, National Aeronautics and Space Administration, Lewis Research Center, Cleveland, Ohio (Mar 1976).

21. Kohl, F. J., B. J. McBride, F. J. Zeleznik, and S. Gordon, "Use of NASA CEC Code for the Prediction of Combustion Gas Deposit Composition," presented at the Spring meeting of the Electrichemical Soc., San Francisco, Calif, U.S.A. (May 8-13, 1983).

22. G. Eriksson, Chemica Scripta, ud 8, p. 100 (1975).

INITIAL DISTRIBUTION

Copies			
2	CONR		
	1	R1232	Allen Roberts
	1	R1232	Wayne Vreatt
5	NAVSEA		
	1	SEA 05D	
	1	SEA 05R23	
	2	SEA 99612	
	1	SEA 56 x 31	
1	NRL 6179		
12	DTIC		

CENTER DISTRIBUTION

Copies	Code	Name
10	2759	R. Strucko
1	2809	
1	281	
2	2812	
30	2813	
1	2803	J. Cavallaro
2	2801	D. Ventriglio
1	284	
1	5211	Knox
1	522.2	TIC (A)
1	5231	Office Services

END

8-87

DTIC